The FRC's n=2 rotational instability interpreted as the dominant Rayleigh-Taylor mode of a gyroviscous plasma with sheared toroidal flow

Edward L. Ruden
Air Force Research Laboratory, Directed Energy Directorate

A Field Reversed Configuration is observed to gain angular momentum until $\alpha = \Omega_R/\Omega_{Di}$ (rotational frequency over ion diamagnetic drift frequency) reaches a critical value, at which point an instability with azimuthal mode number $n = 2$ develops. Questions remain as to whether the observed threshold is explained by published calculations, which assume a rigid rotor profile. Questions also remain as to the cause of the spin-up, but it necessarily involves angular momentum transport to the FRC through the outer surface. Rotation of the bulk, then, via kinematic viscosity and/or convection can entail significant velocity shear. Rotation results in plasma (centripetal) acceleration supported by an external magnetic field, so the instability may be interpreted as a Rayleigh-Taylor mode. Both sheared flow and Finite Larmour Radius effects are recognized as mitigating factors for the R–T instability, and the two effects are synergistic.

The rotational instability is investigated here using an analytic planar R-T model of an FLR plasma with a magnetically transverse sheared flow layer accelerated by the magnetic field. One result is that if the sheared layer is too thin to reach the magnetic (reversal) axis, it is unstable. The coupling between gyroviscosity and flow shear in this case negates the stabilizing effect of both within a range of modes, and convection of the sheared layer to the magnetic axis can be expected to occur quickly. Once this happens, though, the FRC is stable until the shear factor reaches a high value, at which time the $n = 2$ mode goes unstable. Technically, $n = 1$ goes unstable first, but the (planar) model applied to cylindrical geometry does not conserve momentum for this mode, so is unphysical.

This model provides insight into what may be an important feature of FRC stability, although less simplified calculations are needed. Nonetheless, it can be used to tentatively predict stability characteristics of an FRC during compression by an imploding metal cylinder - a goal of the Magnetized Target Fusion program. This is of concern since acceleration from such an implosion supplements centripetal acceleration, and α more than doubles, assuming angular momentum conservation, adiabatic compression, and the expected volume vs. radius scaling.

Introduction

FLR MHD[1], Vlasov[2], and hybrid[3] simulations of the $n = 2$ rotational instability in θ pinches and FRC's to date generally assume the plasma rotates with a rigid rotor profile. The former two are for θ pinches, but relevant to FRC's, and indicate stability up to $\alpha \gtrsim 1$, reasonably consistent with experiment. The hybrid simulation, though, (of an FRC) implies that $n = 2$ should be unstable for $\alpha \gtrsim 0.4$. This significantly lower critical α is attributed to resonant ions near the magnetic axis due to the magnetic field vanishing there - an effect not present in a θ pinch or representable by the FLR stress tensor. The discrepancy with experiment, however, is not well explain. The purpose of this paper is to pose a hypothesis for this discrepancy supported by a simple analytic model and heuristic considerations, pending more detailed analysis.

Little consideration is given in the aforementioned studies as to how a rigid rotor profile develops. The equilibration time scale for Ω_R is

$$\tau_\Omega = \frac{(r_s - r_0)^2}{\nu_k} \qquad \nu_k \left(\frac{\mathrm{m}^2}{\mathrm{sec}}\right) = \frac{3.4 \times 10^2 A_i Z^2 \ln\Lambda}{(ZT_e + T_i)\sqrt{T_i}} \tag{1}$$

where r_s and r_0 are the separatrix and magnetic axis radii, respectively, ν_k is kinematic viscosity[4], Z is mean ionization level, T_i and T_e are ion and electron temperatures in eV, respectively, $\ln\Lambda$ is the Coulomb logarithm, and A_i is the ion atomic mass in amu. For a D_2 plasma with $r_s - r_0 = 1$ cm, $T_i = T_e = 200$ eV, and $\ln\Lambda \approx 15$, typical of MTF FRC's[5], $\tau_\Omega \approx 83$ μs. An $n = 2$ instability, though, is observed to develop within 15 μs of formation.

Faster angular momentum transport schemes have been pro-posed[6]. Indeed, in this paper a mechanism is proposed whereby a sheared flow layer establishes itself between r_s and r_0 on an MHD time scale by convection resulting from the instability of the sheared layer while it is thinner. Once this happens, though, a much more stable shear flow pattern emerges until Ω_R reaches a critical value. Plasma with $r < r_0$ connected to $\mathbf{B}$ field lines within the sheared layer will be carried along at the same Ω_R, but is R-T stable.

The dynamics of the $n = 2$ instability is of particular concern for MTF because α increases significantly during wall compression by a cylindrical liner. To see this, Ω_R goes as r_s^{-2} from angular momentum conservation. Meanwhile, $x_s \equiv r_s/r_c$ is conserved during wall compression, where r_c is the liner inner radius (Tuszewski[7], p. 2058). Given this, plasma β is conserved (Tuszewski, Eq. 10). Given *this* and flux conservation, Ω_{Di} goes as T_i, (Shimamura and Nogi[8], Eq. 7 with $\Omega^* =$

$-\Omega_{Di}$). The FRC's characteristic volume $V = \pi r_s^2 l_s$, meanwhile, goes as r_s^N, where l_s is the separatrix length, and N is the dimensionality of compression. Assuming adiabatic compression, $T_i V^{5/3-1} = \text{const}$. Therefore, $\Omega_{Di} r_s^{2N/3} = \text{const}$, and Ω_{Di} goes as $r_s^{-2N/3}$. α, then, goes as $r_s^{-2}/r_s^{-2N/3} = r_s^{-2(1-N/3)}$. Anything less than 3-D compression, therefore, causes α to increase. Unfortunately, $N = 12/5$ for wall compression (Tuszewski, Table V), so α goes as $r_s^{-2/5}$ or, equilavently, $r_c^{-2/5}$. The (target) factor of 10 radial compression, then, increases α by a factor of $10^{2/5} \approx 2.5$.

The general model used to study the development of the FRC's sheared flow layer is more fully developed in a recent publication[9]. We include a brief summary of its relevant results to make this presentation more self-contained. The model is planar with $\mathbf{x}$, $\mathbf{y}$, and $\mathbf{z}$ directions corresponding to $-\mathbf{r}$, $\boldsymbol{\theta}$, and $\mathbf{z}$ of the FRC's cylindrical coordinates, respectively. The reference frame is rotating, with centripetal acceleration providing "gravity" g.

Model

We assume a perfectly conducting isothermal z invariant plasma with a magnetic field of magnitude B in the $\mathbf{z}$ direction, and a uniform gravitational field of magnitude g in the $-\mathbf{x}$ direction. For incompressible motion confined to the $x-y$ plane, the MHD equation of motion supplemented by the isothermal transverse contribution to the FLR stress tensor $\mathbf{\Pi}$ given by Hazeltine and Meiss[10], Chap. 6, Eq. 123, along with the equations of continuity and state are

$$\begin{gathered}
\rho\partial\mathbf{v}/\partial t + \rho(\mathbf{v}\cdot\boldsymbol{\nabla})\mathbf{v} = -\boldsymbol{\nabla}p^* - g\rho\mathbf{x} - \boldsymbol{\nabla}\cdot\mathbf{\Pi} \qquad \partial\rho/\partial t + \boldsymbol{\nabla}\cdot(\rho\mathbf{v}) = 0 \\
\boldsymbol{\nabla}\cdot\mathbf{v} = 0 \quad p^* \equiv k_B T\rho/m_i + B^2/(2\mu_0) \quad \nu = k_B T_i/(2ZeB) \quad T \equiv (T_i + ZT_e) \\
-(\boldsymbol{\nabla}\cdot\mathbf{\Pi})\cdot\mathbf{x} = \frac{\partial}{\partial x}\left[\nu\rho\left(\frac{\partial v_y}{\partial x} + \frac{\partial v_x}{\partial y}\right)\right] - \frac{\partial}{\partial y}\left[\nu\rho\left(\frac{\partial v_x}{\partial x} - \frac{\partial v_y}{\partial y}\right)\right] \\
-(\boldsymbol{\nabla}\cdot\mathbf{\Pi})\cdot\mathbf{y} = -\frac{\partial}{\partial y}\left[\nu\rho\left(\frac{\partial v_y}{\partial x} + \frac{\partial v_x}{\partial y}\right)\right] - \frac{\partial}{\partial x}\left[\nu\rho\left(\frac{\partial v_x}{\partial x} - \frac{\partial v_y}{\partial y}\right)\right]
\end{gathered} \tag{2}$$

$\mathbf{v}$, ρ, m_i, μ_0, k_B, e, and ν are velocity, density, ion mass, free space permeability, Boltzmann constant, elementary charge, and gyroviscosity coefficient, respectively.

The equilibrium states of interest have $\mathbf{v} = V(x)\,\mathbf{y}$, $\rho = \rho_0(x)$, $\mathbf{B} = B_0(x)\,\mathbf{z}$, and $\nu = \nu_0(x)$. For instabilities with short wavelengths relative to the sheared flow layer thickness, consider case I of two semi-infinite regions separated at $x = 0$ with equilibrium conditions

$$\begin{array}{llll}
\rho_0 = \rho_1 & V = s_1 x & \nu_0 = \nu_1 & \text{if} \quad x < 0 \\
\rho_0 = \rho_2 & V = s_2 x & \nu_0 = \nu_2 & \text{if} \quad x \geq 0
\end{array} \tag{3}$$

where ρ_1, ρ_2, s_1, s_2, ν_1, and ν_2 are constants. Assuming shear factors within bounds easily met in fusion research relevant FRC's ($s \ll 4ZeB/\left(\beta_i m_i\right)$, where β_i is the ion pressure to magnetic pressure ratio), the condition for linear instability of a perturbation with $\exp(i\omega t + iky)$ dependence, implying maximum growth rate $\gamma = \max\left(-\operatorname{Im}\omega\right)$, is

$$J^* > \frac{\left(1-G^*K^2\right)^2}{2K} \rightarrow \Gamma = \sqrt{1-\frac{\left(1-G^*K^2\right)^2}{2J^*K}} \quad J^* \equiv \frac{g^*}{s^{*2}d} \quad G^* \equiv \frac{\nu^*}{2s^*d^2} \quad \Gamma \equiv \frac{\gamma}{\sqrt{g^*k}} \qquad (4)$$
$$K \equiv 2kd \quad \nu^* = \frac{\nu_2\rho_2 - \nu_1\rho_1}{\rho_1+\rho_2} \quad s^* = \frac{s_2\rho_2 - s_1\rho_1}{\rho_1+\rho_2} \quad g^* = g\frac{\rho_2-\rho_1}{\rho_1+\rho_2}$$

Here, $2d$ is the thickness of the plasma layer intended to be modeled. An R-T relevant configuration is one for which $\rho_2 > \rho_1$, implying positive J^*. G^* may be of either sign regardless of the relative magnitudes of ρ_1 and ρ_2. The global stability criterion is

$$J^* \leq \begin{cases} 8\sqrt{-G^*/27} & \text{if} \quad G^* < 0 \\ 0 & \text{if} \quad G^* \geq 0 \end{cases} \qquad (5)$$

Note that an R-T relevant configuration is unstable if $G^* > 0$, and gyroviscosity suppresses the stabilizing influence of flow shear in the vicinity of $K = 1/\sqrt{G^*}$.

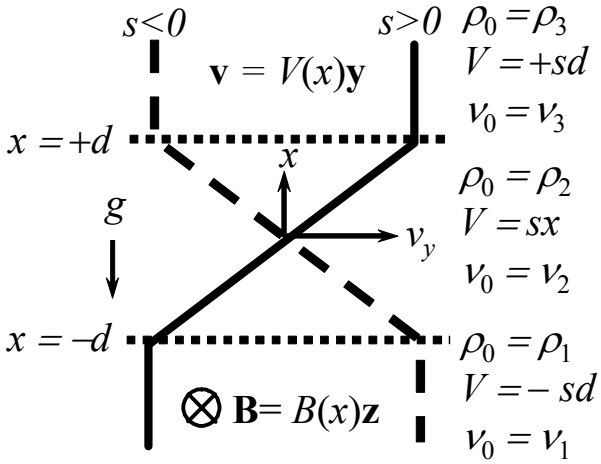

Fig. 1 Geometry and coordinate system assumed for case II - a flow sheared layer separating two unsheared semi-infinite regions. The $\otimes$ "tail feathers" symbol indicates the magnetic field direction is into the page. The solid/dashed V vs. x plot corresponds to a positive/negative shear factor s, given the coordinate conventions.

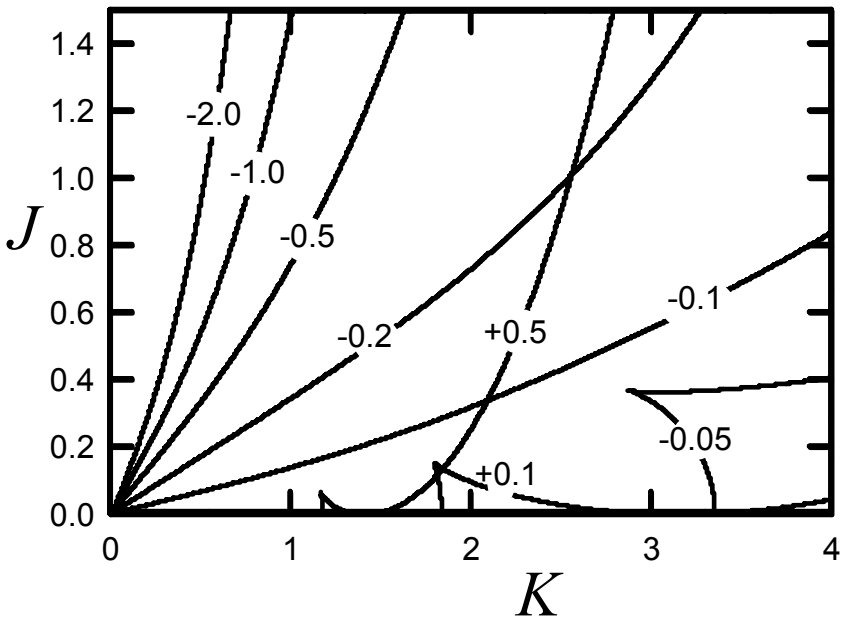

Fig. 2 Stability boundaries for case II with $\epsilon_1 = \epsilon_3 = 0$ for various values of G_2. The stable region is to the right and below each contour. Note for $G_2 > 0$, the value of K unstable for all J is $K = 1/\sqrt{G_2}$, the same as with case I with $G^* = G_2$.

For case II, we assume three regions of uniform ρ_0 and ν_0 with equilibrium properties identified by subscripts 1, 2, and 3. We restrict uniform flow shear to the intermediate region of thickness $2d$, and drop the "$*$" superscripts used to generalize the results. As Illustrated in Fig. 1, In equilibrium,

$$\begin{array}{llll} \rho_0 = \rho_1 & V = -sd & \nu_0 = \nu_1 & \text{if} \quad x < -d \\ \rho_0 = \rho_2 & V = sx & \nu_0 = \nu_2 & \text{if} \quad -d < x < +d \\ \rho_0 = \rho_3 & V = +sd & \nu_0 = \nu_3 & \text{if} \quad x > +d \end{array} \tag{6}$$

The linear dispersion relation this time is a quartic ω with solutions parameterized parameterized by

$$K \equiv 2kd \quad J \equiv \frac{g}{s^2 d} \quad G_i \equiv \frac{\nu_i}{2sd^2} \quad \epsilon_i \equiv \frac{\rho_i}{\rho_2} \tag{7}$$

Figure 2 plots the stability boundaries for $\epsilon_1 = \epsilon_3 = 0$ for a G_2 range relevant to FRC's. This represents a plasma layer accelerated by a $\mathbf{B}$ field.

FRC application

We now relate this model to an FRC. The ion diamagnetic drift frequency is

$$\Omega_{Di} = -\frac{v_{Di}}{r} \qquad \mathbf{v}_{Di} = -\frac{\boldsymbol{\nabla} p_i \times \mathbf{B}}{eZn_iB^2} \tag{8}$$

where $\mathbf{v}_{Di}$ is diamagnetic drift velocity, p_i and n_i are ion pressure and number density, respectively, and we take the external magnetic field $\mathbf{B}$ to be in the $\mathbf{z}$ direction. The exterior pressure scale length is $(r_s - r_0)$. We take the characteristic Ω_{Di} to be, with the help of Eqs. 2, then,

$$\Omega_{Di} = -\frac{2A\nu}{r_0^2} \quad A = \frac{r_0}{r_s - r_0} \qquad r_s = r_0\frac{1+A}{A} \tag{9}$$

where A is a measure of the FRC aspect ratio.

Consider now a sheared flow layer that has diffused distance $2d$ into the FRC. The angular velocity is Ω_R at $r = r_s$, dropping to zero at $r = r_s - 2d$. One shortcoming of applying the planar model to an FRC is that centripetal acceleration depends on r, while the model assumes g is constant. With the understanding that we are only seeking rough estimates of mode behavior, we'll take our characteristic g to be half its peak value. And, since g goes as Ω_R^2, we'll take the characteristic angular velocity for the purposes of defining α to be $\Omega_R/\sqrt{2}$,

$$g = \frac{\Omega_R^2 r_s}{2} \qquad \alpha \equiv \frac{\Omega_R}{\sqrt{2}\Omega_{Di}} \tag{10}$$

It should be noted, though, that these expressions are only appropriate for low order n modes which are not localized to either inner or outer boundary. The characteristic g will be somewhat higher for high order modes localized to the outer surface, and lower for interior modes.

Meanwhile, the surface speed is $2V = \Omega_R r_s$, and the layer's shear factor is $s = V/d$. So, with the help of Eqs. 9,

$$\Omega_R = \frac{sA}{A^*(1+A)} \qquad A^* = \frac{r_0}{2d} \tag{11}$$

Where A^* is the aspect ratio of the sheared layer. From Eqs. 9 and Eqs. 10, then,

$$G_2 \equiv \frac{\nu}{2sd^2} = -\frac{A^*}{\sqrt{2}\alpha(1+A)} \tag{12}$$

This provides G_2 for case II, and a way to find G^* for case I as applied to high n modes localized to the *inner* shear layer boundary. Note that for an FRCs, Ω_R develops with the same sign as Ω_{Di}[11] ($\alpha > 0$). Therefore, s and G_2 here are negative.

From Eqs. 10 and Eqs. 11,

$$J = \frac{g}{s^2 d} = \frac{A}{A^* (1 + A)} \tag{13}$$

This provides J for case II. Meanwhile, to relate mode number n to the model, we use $k = n/r_0$. From Eqs. 11, then,

$$K = 2kd = \frac{n}{A^*} \tag{14}$$

Thin shear layer

As an application of case I, consider a shear layer represented by region 1 which has diffused a small distance into the FRC ($A^* \gg A$). The interior is taken to be region 2 with $s_2 = 0$ and a higher density of, say, $\rho_2 = 2\rho_1$. B is fairly uniform in the vicinity of interest, so $\nu_2 = \nu_1$ is assumed. From Eqs. 4,

$$\nu^* = \frac{\nu_1}{2} \quad s^* = -\frac{s_1}{3} \quad g^* = \frac{g}{3} \quad J^* = 3\left(\frac{g}{s_1^2 d}\right) \quad G^* \equiv -\frac{3}{2}\left(\frac{\nu_1}{2 s_1 d^2}\right) \tag{15}$$

The natural spin-up of an FRC results in $s_1 < 0$, so $G^* > 0$. From Eq. 5, then, the configuration is unstable with least stable mode $K = 1/\sqrt{G^*}$. From Eq. 15, Eq. 12, and Eq. 14, this corresponds to

$$n = \sqrt{\frac{2\sqrt{2}}{3}}\sqrt{\alpha A^* (1 + A)} \approx \sqrt{\alpha A^* (1 + A)} \tag{16}$$

For example, if $A = 2$, $A^* = 10$, and $\alpha = 1$, the least stable mode is $n = 5$.

The FRC must survive this turbulent period where unstable modes become of increasingly lower order as the FRC settles down and A^* decreases. Experimental conditions for this to occur successfully are determined empirically. Framing camera images in visible light during the early θ pinch phase of FRC formation[12], and in VUV during early reversal[13] often show high order mode activity, for which the above model may provide a qualitative description. Convective transport of angular momentum toward the interior can be expected on an MHD time

scale until the shear layer reaches $r = r_0$ ($A^* = A$), where $G^* > 0$ is no longer the case. We treat this phase below.

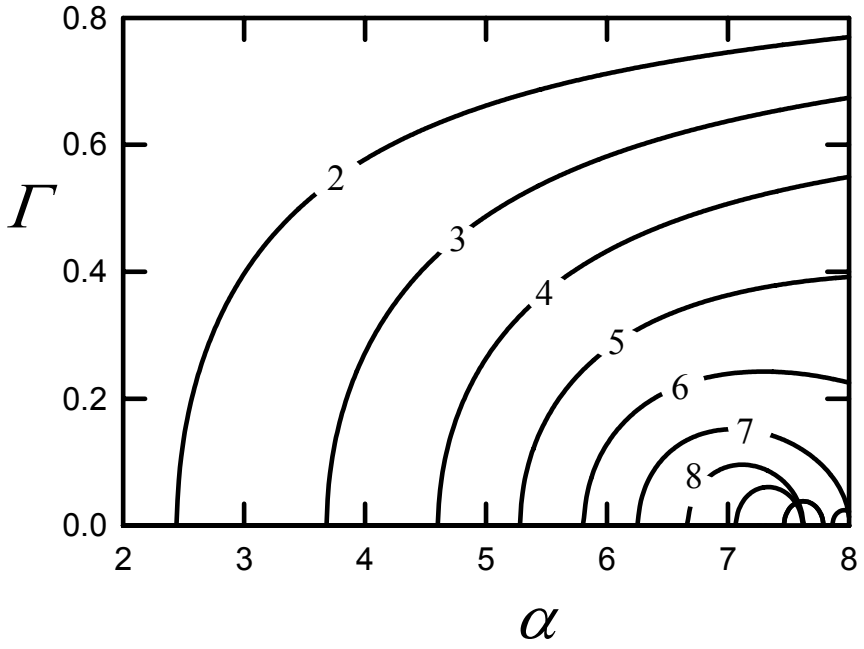

Fig. 3 Normalized growth rate Γ vs α for various modes n (labeled) for $A = 2$.

Thick shear layer

Assuming a well sheared layer diffused to r_0 ($A^* = A$), case II parameters are, from Eq. 12, Eq. 13, and Eq. 14,

$$G_2 = -\frac{A}{\sqrt{2}\alpha\,(1+A)} \qquad J = \frac{1}{(1+A)} \qquad K = \frac{n}{A} \tag{17}$$

Figure 3 illustrates the growth rate vs. α for the first several modes with $A = 2$. These normalized curves have a very weak dependence on A, though, for low n. The stability threshold for $n = 2$ in the rage $1 \leq A \leq 4$ is $\alpha = 2.5 \pm 0.1$.

Rigid rotor limit

Shortcomings of the presented model include the finiteness of A^* (planar geometry is best reserved for high aspect ratio), the nonuniformity of properties within the sheared layer (especially centripetal acceleration), and the Coriolis effect. A *relative* comparison the stability characteristics of an FRC with a thick sheared flow layer vs. one rotating as a rigid rotor using our model is, therefore, instructive. For this, we use our case I results to estimate the stability threshold and growth rate of a rigid rotor. Taking region 1 and 2 now to represent the plasma exterior and interior, respectively, we have from Eqs. 4,

$$s_1 = s_2 = \rho_1 = \nu_1 = 0 \qquad \nu^* = \nu_2 \qquad s^* = 0 \quad g^* = g \tag{18}$$

Equations 4 in the limit $s^* \to 0$, then, imply

$$g > \nu_2^2 k^3 \to \gamma = \sqrt{gk - \nu_2^2 k^4} \tag{19}$$

Relating this to FRC properties as before, but without corrections to g and α motivated by shear, we get

$$g = \Omega_R^2 r_s \quad \alpha = \frac{\Omega_R}{\Omega_{Di}} \quad k = \frac{n}{r_0} \quad \Omega_{Di} = -\frac{2A\nu_2}{r_0^2} \tag{20}$$

and Eq. 19 becomes

$$|\alpha| > \sqrt{\frac{n^3}{4A\left(1+A\right)}} \to \frac{\gamma}{\Omega_{Di}} = \sqrt{\frac{\left(1+A\right)n\alpha^2}{A} - \frac{n^4}{4A^2}} \tag{21}$$

For $n = 2$ and $A = 2$, this is

$$|\alpha| > 0.58 \to \frac{\gamma}{\Omega_{Di}} = \sqrt{3\alpha^2 - 1}$$

Therefore, independent of the absolute accuracy of our model, it implies substantially greater stability if an FRC's angular momentum is the result of a thick flow sheared layer vs. a rigid rotor.

To assess the absolute accuracy of the model, we use case I to represent a θ pinch of radius R rotating at frequency Ω_R, but without shear, and compare it to published FLR MHD calculations of the linear mode structure of a rigidly rotating

θ pinch[1]. Proceeding as above, but with R as the only relevant radius *and* the radial gradient scale length for Ω_{Di},

$$g = \Omega_R^2 R \quad \alpha = \frac{\Omega_R}{\Omega_{Di}} \quad k = \frac{n}{R} \quad \Omega_{Di} = -\frac{2\nu_2}{R^2} \tag{22}$$

and Eq. 19 becomes

$$|\alpha| > \frac{n^{\frac{3}{2}}}{2} \rightarrow \frac{\gamma}{\Omega_{Di}} = \sqrt{n\alpha^2 - \frac{n^4}{4}} \tag{23}$$

For $n = 2$, this is

$$|\alpha| > \sqrt{2} \rightarrow \gamma/\Omega_{Di} = \sqrt{2\alpha^2 - 4} \tag{24}$$

Freidberg and Perlstein's[1] Fig. 8 shows that the $n = 2$ mode in a θ pinch with a more realistic profile with $\beta_0 \rightarrow 0$, as they define it, is unstable if $\alpha > 1.2$ *or* $\alpha < -0.2$ ($\Omega_{Di} = -\Omega^*$). Our model best describes the low β limit since we do not account for variations in the magnitude of B. For a uniform density θ pinch with an abrupt drop to zero density at a given radius (much as we assume), we find from F-P Eq. 41 that $n = 2$ is unstable for $\alpha > 1.8$ or $\alpha < -0.3$ in the low β limit. The proximity of these thresholds to ours for positive α suggests our $\alpha = 2.5 \pm 0.1$ threshold may indeed be a reasonable estimate of the effect of gyroviscosity on an FRC with a thick shear layer with $\alpha > 0$. One discrepancy is that our model makes a distinction for the sign of α in the flow sheared case, but not for a rigid rotator, while F-P's results imply $\alpha > 0$ is more stable for the later. The reason for this is that while our planar model treats the effects of centripetal acceleration, it neglects the Coriolis effect.

Conclusions

Substantially lower values of α are observed experimentally than can be explained by FLR MHD theory in the context of the presented model where angular momentum is the result of a thick flow sheared layer between the separatrix and magnetic axis of an FRC. One possible explanation suggested by published hybrid simulations[3] is that resonant ions (not represented by FLR MHD) near the magnetic axis reduce stability well below the $\alpha = 2.5$ value of our model. If this is the case, it may be possible to substantially increase the critical α in FRC experiments if resonant ions can be damped by, for example, introduction of a small toroidal magnetic field.

References

[1] J. P. Freidberg and L. D. Pearlstein, Phys. Fluids **21**, 1207 (1978).

[2] C. E. Selyer, Phys. Fluids **22**, 2324 (1978).

[3] D. S. Harned, Phys. Fluids **26**, 1320 (1981).

[4] L. Spitzer Jr., *Physics of Fully Ionized Gases* (John Wiley & Sons, New York, NY, 1967).

[5] T. Intrator, S. Y. Zhang, J. H. Degnan, I. Furno, C. Grabowski, S. C. Hsu, E. L. Ruden, P. G. Sanchez, J. M. Taccetti, M. Tuszewski, W. J. Waganaar, and G. A. Wurden, Phys. Plasmas **11**, 2580 (2004).

[6] L. C. Steinhauer, Phys. Fluids **24**, 328 (1981).

[7] M. Tuszewski, Nuclear Fusion **28**, 2033 (1988).

[8] S. Shimamura and Y. Nogi, Fusion Tech. **9**, 69 (1978).

[9] E. L. Ruden, Phys. Plasmas **11**, 713 (2004).

[10] R. D. Hazeltine and J. D. Meiss, *Plasma Confinement* (Addison-Wesley, Redwood, CA, 1992).

[11] M. Tuszewski, Phys. Fluids B **2**, 2541 (1990).

[12] T. P. Intrator, J. Y. Park, J. H. Degnan, I. Furno, C. Grabowski, S. C. Hsu, E. L. Ruden, P. G. Sanchez, J. M. Taccetti, M. Tuszewski, W. J. Waganaar, G. A. Wurden, S. Y. Zhang, and Z. Wang, IEEE Trans. on Plasma Sci. **32**, 152 (2004).

[13] D. P. Taggart, R. J. Gribble, A. D. Bailey III, and S. Sugimoto, in *US-Japan Workshop on Field-Reversed Configurations with Steady-State High-Temperature Fusion Plasmas and the 11'th US-Japan Workshop on Compact Toroids*, edited by D. C. Barnes, J. C. Fernández, and D. J. Rej (LANL, LA-11808-C, Los Alamos, NM, 1994), pp. 87–92.